DOI: 10.24996/ijs.2025.66.5.25

ISSN: 0067-2904

# Seasonal Effects of Environmental Factors on the Performance Parameters of Three Types of Silicon Solar Modules at NRIAG, Helwan, Egypt

**Heba Zenhom[1*], Ahmed Ghitas[1], Ahmed Abulwfa[1], Maha Harhash[2], M S El-Nawawy[2], Mohamed M. Abdelwahab[2]**

*[1]Solar and Space Research Department, National Research Institute of Astronomy and Geophysics (NRIAG), Helwan, Egypt*

*[2]Astronomy, Space Sciences and Meteorology Department, Faculty of Science, Cairo University, Giza, Egypt*

Received: 11/1/2024 Accepted: 16/4/2024 Published: 30/5/2025

**Abstract**

The performance of PV modules, which is evaluated under standard test conditions, rarely meets actual outdoor conditions due to the fluctuations of PV output readings. The present work investigates the behavior of performance parameters of three PV technologies, namely mono-crystalline, poly-crystalline, and amorphous, under variation of environmental factors (ambient temperature Ta, relative humidity R.H., and solar irradiance G) in the four seasons on clear sky days during the year 2021. The performance parameters include open circuit voltage Voc, short circuit current density Jsc, ideal output power density PD, and ideal efficiency ηo. The study employed the first-designed I-V logger as a prototype for data collection at the Helwan site. The results revealed that all electrical performance parameters of the three solar modules have seasonally changed with environmental factors. In this sense, the performance parameters of three modules were strongly affected by the temperature coefficient of conversion efficiency in the afternoon period of the day. As a result, the highest values of depression in the ideal efficiency (ηo) due to the effect of ambient temperature (Ta) were -0.6%, -0.57%, and -0.3% for mc-Si, pc-Si, and a-Si, respectively during the afternoon period in the summer season. While the greatest percentage drops in ηo values of mc-Si, pc-Si, and a-Si were -0.87%, -0.78%, and -0.32%, respectively, per unit increase in relative humidity (R.H.) over the winter. On the other hand, the performance of crystalline Si PV technologies is more affected by solar irradiance than a-Si technology in the winter season. The obtained results provide a comprehensive understanding of the operating behavior of each solar PV module type, which will be utilized to optimize the PV power system at the considered site in the future.

**Keywords**: Environmental Factors, Solar PV Modules, Performance Parameters, Efficiency

# التأثيرات الموسمية للعوامل البيئية على معايير الأداء لثلاثة أنواع من وحدات الطاقة الشمسية السيليكونية في NRIAG، حلوان، مصر

**هبه زينهم[1*]، احمد غيطاس[1]، احمد ابو الوفا[1]، مها حرحش[2]، محمد صالح النواوي[2]، محمد مجدي عبدالوهاب[2]**

[1]قسم أبحاث الطاقة الشمسية والفضاء، المعهد القومي للبحوث الفلكية والجيوفيزيقية (NRIAG) ، حلوان، مصر

[2]قسم علوم الفلك، علوم الفضاء والأرصاد الجوية، كلية العلوم، جامعة القاهرة، الجيزة، مصر

*Email: heba.zenhom@nriag.sci.eg

**الخلاصة**

يتم تقييم أداء الوحدات الكهروضوئية في ظل ظروف الاختبار القياسية، والتي نادراً ما تلبي الظروف الخارجية الفعلية وذلك لاختلاف إنتاج الطاقة الكهروضوئية في كثير من الأحيان. يبحث العمل الحالي في سلوك معاملات الأداء لثلاث تقنيات كهروضوئية، وهي أحادية التبلور، ومتعددة التبلور، وغير متبلورة، في ظل تباين العوامل البيئية (درجة الحرارة المحيطة Ta والرطوبة النسبية R.H. والإشعاع الشمسي G) في الفصول الأربعة في أيام صافية خلال عام 2021. وتشمل هذه المعاملات جهد الدائرة المفتوحة Voc، وكثافة تيار الدائرة القصيرة Jsc، وكثافة طاقة الخرج المثالية PD، والكفاءة المثالية ηo. استخدمت الدراسة أول جهاز تسجيل I–V كنموذج أولي لجمع البيانات في موقع حلوان. أظهرت النتائج أن جميع معايير الأداء الكهربائي للوحدات الشمسية الثلاثة قد تغيرت موسمياً مع العوامل البيئية. تأثرت معاملات الأداء لثلاث وحدات بشدة بمعامل درجة الحرارة لكفاءة التحويل في فترة ما بعد الظهر من اليوم. توفر النتائج التي تم الحصول عليها فهمًا شاملاً لسلوك التشغيل لكل نوع من وحدات الطاقة الشمسية الكهروضوئية، والتي سيتم استخدامها لتحسين نظام الطاقة الكهروضوئية في الموقع المعني في المستقبل.

## 1. Introduction

Recently, the amount of solar energy that reaches the Earth's surface has become crucial for many different scientific and engineering purposes. Studies on climate change, the monitoring of air pollution, and photovoltaic (PV) devices are a few examples of these uses [1, 2]. The performance of a solar photovoltaic module is dependent upon many site-specific factors, such as latitude, season, cloudiness, and air pollution [3, 4]. Typically, PV product suppliers and manufacturers provide the data that is measured based on standard test conditions. Usually, these standard test conditions (STC) are not always representative of the actual operation of a PV module. This is attributed to the fact that the performance of these solar PV modules may decline after being exposed to outdoor field conditions. This decline in the performance of the PV modules is due to the change in weather conditions from one environment to another and is amplified by the effect of the aging of the PV modules [5-7]. Since PV modules experience seasonal variations throughout the year, it is important to characterize different types of PV modules under real operating conditions in order to provide a comprehensive view of the actual electrical performance of different technologies at a specific site [3, 8, 9]. The main environmental factors that affect the performance and efficiency of PV modules are ambient temperature, solar radiation, and relative humidity [10-13].

Many studies have been conducted to determine how different environmental factors affect the performance of PV systems. Touati et al. investigated the proneness of certain solar photovoltaic systems to Doha's climate's relative humidity. The investigation revealed that as the PV panel's relative humidity increased beyond the minimal value of 22%, the panel’s output decreased. On the other hand, changes in relative humidity above 22% had a greater impact on amorphous PVs. This implied that monocrystalline PVs might be more beneficial than amorphous PVs in the Doha situation [14]. The performance of three commercially available solar modules (monocrystalline, polycrystalline, and single junction amorphous silicon) was compared by Bashir et al. in Taxila, Pakistan. Wintertime outside conditions were used for the experimentation. Power output, module efficiency, and performance ratio all displayed significant irradiance and temperature sensitivity [15].

Ramgolam et al. tested how various solar cell technologies performed in relation to solar irradiation. The study found that while solar irradiance had little impact on the voltage parameters, it had a significant impact on the current parameters. Additionally, it was discovered that thin film technology displayed a lower reaction to irradiance than wafer-based technology [16].

WanQuan et al. researched how the electrical properties of a polycrystalline solar PV panel behaved when temperature and sun irradiation varied in the springtime. Due to favourable surface temperature and solar irradiance changes hitting the module during the day's peak hours, the PV module's output was more efficient during the spring season as a result of these two variables [17]. The impact of temperature and humidity on the performance of the polycrystalline solar panel was demonstrated by Baraya et al. The result obtained shows that voltage production remains relatively stable with a temperature below 42ºC and humidity below 60%, while power production is fairly stable with a humidity below 40% and a maximum temperature of 45ºC. Current production is greatly aided by temperatures within 42-45ºC and humidity below 35% [18]. The influence of seasonal ambient temperature variations on the ideal PV panel tilt angle in the United States has been realized by Alhamer et al., in their work. According to the findings, hot summer weather, particularly in southern areas, lowers panel efficiency [9].

The aim of this work is to present the effects of temperature $T_a$, relative humidity R.H., and solar irradiance G on different PV technologies: "mono-crystalline (mc-Si), polycrystalline (pc-Si), and amorphous (a-Si)" that change from season to season. For this reason, an experimental study of the physical behavioral mechanisms of three PV modules was carried out. The used data are based on outdoor measurements on selected clear days. As a result, the rates of PV module efficiency growth and decline fluctuate from season to season and from period to period during the day. We propose that location-specific, measurable qualification standards for the testing of PV modules should be established. This can be achieved after a comprehensive analysis of environmental factors at each interval of time during different seasons. Hence, improving the design and operating performance of PV modules.

## 2. Methodology

### 2.1. Data collection

The experiment was conducted at the National Research Institute of Astronomy and Geophysics (NRIAG) in Helwan, Egypt (Lat. 29. 866 N, Long. 31. 20 E, and 130 m above sea level). All measurements were taken during the period from January 1 to December 31, 2021. During this period, the regular daily measurements of the environmental factors ambient air temperature ($T_a$), solar irradiance (G), and relative humidity (R.H.) were also recorded. The electrical performance parameters of the PV modules were evaluated and statistically analyzed. These parameters included open circuit voltage $V_{oc}$, short circuit current density $J_{sc}$, output ideal power density $P_D$, and ideal efficiency $\eta_{o.}$ The evaluation of the performance parameters was conducted on clear sky for four days. These four days were chosen to represent the four seasons of the year 2021. That means January 7 was selected for winter, April 8 for spring, July 7 for summer, and October 5 for autumn, as mentioned in the previously published work [19].

### 2.2. Meteorological conditions

The climate around the site of Helwan City is hot, dry, and dusty. It is characterized by four seasons: summer and winter are classified as traditional seasons, while spring and autumn are classified as transitional seasons. In addition, Helwan is an industrialized town that is affected by the existence of significant sources of pollution in the west, including a power station and Port Land Cement Company, in the southwest. Therefore, these pollution sources have an impact on the observational conditions at this site [19]. In Helwan, the daily average temperature varies from 37.7 $^{O}$C in July to 18.3 $^{O}$C in January. Between 64% in July and 83% in January, the relative humidity varies, and there is about a 5-kilometre visibility range. During such meteorological conditions, the reduced solar radiation is occasionally caused by an increase in water vapor, occasionally by an increase in aerosol particles, and occasionally by a combination of both of these factors.

### 2.3. Instrumentation

#### 2.3.1. PV modules

In this study, three different types of silicon solar modules (mc-Si), (pc-Si), and (a-Si) were used for the experiment. These modules were mounted on a fixed, tilted holder. The holder was mounted facing south at an inclination of 32°, which is the optimum tilt angle of the site, while the output terminals of the modules were connected to the input terminals of the NRIAG I-V logger. Figure 1 shows the field test equipment for three PV modules used during the experiment: (a) amorphous module; (b) poly-crystalline module; (c) mono-crystalline module. The specifications of the three PV modules are illustrated in Table 1.


**Figure 1:** Field test equipment for three Si modules: (a) amorphous module, (b) poly-crystalline module, and (c) mono-crystalline module

**Table 1: Specifications of PV modules at STC (1000 W/m2, AM1.5, 25 °C)**

| Module Type / Parameter | Mono-crystalline silicon | Poly-crystalline silicon | Amorphous silicon |
|---|---|---|---|
| **Power (W)** | 85 | 120 | 9 |
| **$V_{max}$ (V)** | 17.6 | 16.49 | 22.59 |
| **$I_{max}$ (A)** | 4.82 | 7.24 | 0.41 |
| **Open circuit voltage ($V_{oc}$)** | 21.6 | 16.73 | 22.78 |
| **Short circuit current ($I_{sc}$)** | 5.21 | 8.97 | 0.49 |
| **Module Area ($m^2$)** | 0.527 | 0.698 | 0.261 |

### 2.3.2. NRIAG I-V logger

Monitoring and recording of solar module parameters (open-circuit voltage $V_{oc}$ and short-circuit current $I_{sc}$) have been done by designing a multi-channel prototype. This prototype, namely the NRIAG I-V logger, was designed by the authors using an Arduino Mega 2560 microcontroller at NRIAG. Using Arduino programming, the circuit was programmed to read short-circuit current Isc, open-circuit voltage Voc, and temperature T automatically even on the weekend and official holidays. These parameters were used directly to characterize the performance of the modules and describe their behavior under varying environmental factors. The NRIAG I-V logger is shown in Figure 2. The output behavior of the three modules was recorded every 10 minutes of the experiment. Microsoft Excel was used to plot the characteristics of the output graphs of the module parameters.


a b

**Figure 2: (**a) Construction of the NRIAG I-V logger for current and voltage measurements, (b) NRIAG I-V logger internal components

### 2.3.3. Davis weather station

The Davis weather station (Vantage Pro 2) contains two parts: the Integrated Sensor Suite (ISS) that collects outside weather data and the Vantage Pro2 console that receives wireless data from the ISS. The ISS contains a temperature sensor, a humidity sensor, and a solar radiation sensor. The Vantage Pro 2 records data every 10 minutes. The outdoor measurement setup is shown in Figure 3.

**Figure 3:** Outdoor measurement setup

### 2.4. Data analysis

To calculate the PV module's output power, we use the following Eq. (1):

$$P = IV \text{……………. Eq.} \quad (1)$$

Where V and I are the module voltage (V) and current (A), respectively. Since the solar module can be operated in short circuit and open circuit, as in our experiment, $P_{out}$ can be taken to be the ideal power $P_o$, where $P_o = V_{oc} I_{sc}$. Hence, by calculating the efficiency, which is the ratio of the output electrical power $P_{out}$ compared to the input solar power $P_{in}$, in the PV module, we can get the ideal efficiency, as follows in Eq. 2.

$$\eta = P_{out} / P_{in} \quad \eta_o = P_o / P_{in} \text{……………………… Eq} \quad (2)$$

Where $P_{in}$ is taken as the product of the incident solar irradiance, measured in W/m$^2$, with the surface area of the solar module (m$^2$). The ideal efficiency of a PV module can be calculated using Eq. 3:

$$\eta_o\,(PV) = ((V_{oc} * I_{sc})/(G * A)) * 100\% = ((P_o)/(G * A)) * 100\% \text{... Eq.} \quad (3)$$

Where G refers to global solar irradiance (W/m$^2$) and A refers to module area (m$^2$) [20-22]. To evaluate the statistical behavior and correlation of data, we use the following mathematical formula in Eq. 4:

**Simple linear regression:**

$$y = b + ax \text{ …………Eq.} \quad (4)$$

Where *x* is the value of the independent variable, *y* is the predicted value of the dependent variable, *b* is a constant, and *a* is the regression coefficient.

## 3. Results and discussion

The results of three PV modules for the selected clear days in the four seasons were presented in order to study the environmental effects on the performance parameters of the PV modules. Hence, we could determine how these environmental factors affect the output power and efficiency of PV. This has been achieved in two parts: first, the behavior of the three PV modules has been shown in detail and plotted in figures during the spring season as an example before introducing tables to investigate how efficiently PV performance parameters changed over the other seasons.

### Part I: Effects of Environmental Factors on the Performance Parameters of the Three PV Modules in the Spring Season

### 3.1. Ambient temperature dependence of module's performance parameters

One of the key environmental factors for evaluating the performance of a PV module is the ambient air temperature. In this section, the PV characteristics were analyzed at different temperature levels, as shown in Figures 4 to 6. Increasing temperature reduces the band gap of a solar module, affecting the module's electrical parameters, such as open circuit voltage ($V_{oc}$), short circuit current ($I_{sc}$), output power (P), and efficiency ($\eta$) [23, 24]. This is evident from the experimentation that was done by measuring the characteristics of solar modules at various temperatures. Regression analyses were carried out to determine the dependence of these electrical performance parameters on the ambient air temperature ($T_a$) for mc-Si, pc-Si, and a-Si. To ignore the dependence on each cell area of the three solar modules, it is more typical to mention the short-circuit current density ($J_{sc}$ in mA/cm$^2$) and ideal power density ($P_D$ in mW/cm$^2$). The graphs in Figures 4 to 6 show the effect of $T_a$ on $V_{oc}$, $J_{sc}$, $P_D$, and ideal efficiency $\eta_o$ in April (spring season). Based on the time of day, the data in Figure 4 can be divided into three periods: the first one is from the sun rising up to 8:00 a.m., in which the rate of increase is rapid. The second one is from 8:00 a.m. to 4:00 p.m., a period with small depressions in the $V_{oc}$ values. The maximum of these depressions occurs approximately 2 hours after midday, when $T_a$ is at its highest. This period is practically considered a constant period for the change rate. The third one, in which the $V_{oc}$ is observed to decrease sharply with an increase in $T_a$ from 4:00 p.m. until sundown. Similar results have been shown by Sun WanQuan et al [17]. In the case of mc-Si, pc-Si, and a-Si, the obtained $V_{oc}$ data demonstrate that the stability process for $V_{oc}$ is close 20.25 to 20.69 V, 16.51 to 16.88 V, and 22.01 to 22.59 V at outdoor settings, respectively. This can be attributed to the maximum voltage capacity of the solar module, which depends on the forbidden gap of each PV technology. The rate of change of the $V_{oc}$ of the three modules varies according to each module technology, as shown in Figure 4. Compared to the wafer technologies of mc-Si and pc-Si, the thin film technology a-Si has a larger rate of change in $V_{oc}$.

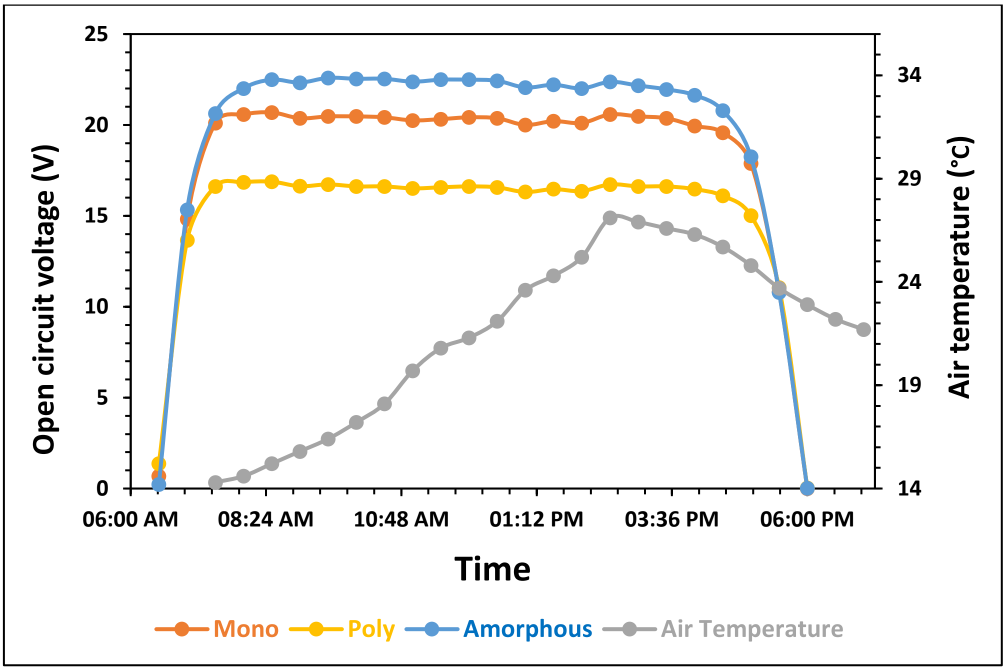


**Figure 4:** The daily profiles of $V_{oc}$ of the three modules mc-Si, pc-Si, and a-Si and $T_a$ (°C) on the experimental day in April

On the other side, the performance parameters, $J_{sc}$, $P_D$, and $\eta_o$, are plotted in Figures 5 (a, b, c) and 6 (a, b, c) as a function of $T_a$ in the periods of before noon and afternoon, respectively. Figure 5a shows that $J_{sc}$ increases due to the rise in $T_a$ before noon. This leads to an increase in the $P_D$, and consequently, $\eta_o$ also increases during the before noon period, as shown in Figures 5b and c, respectively. Similar results have been found in previously published work [11, 17, 18].

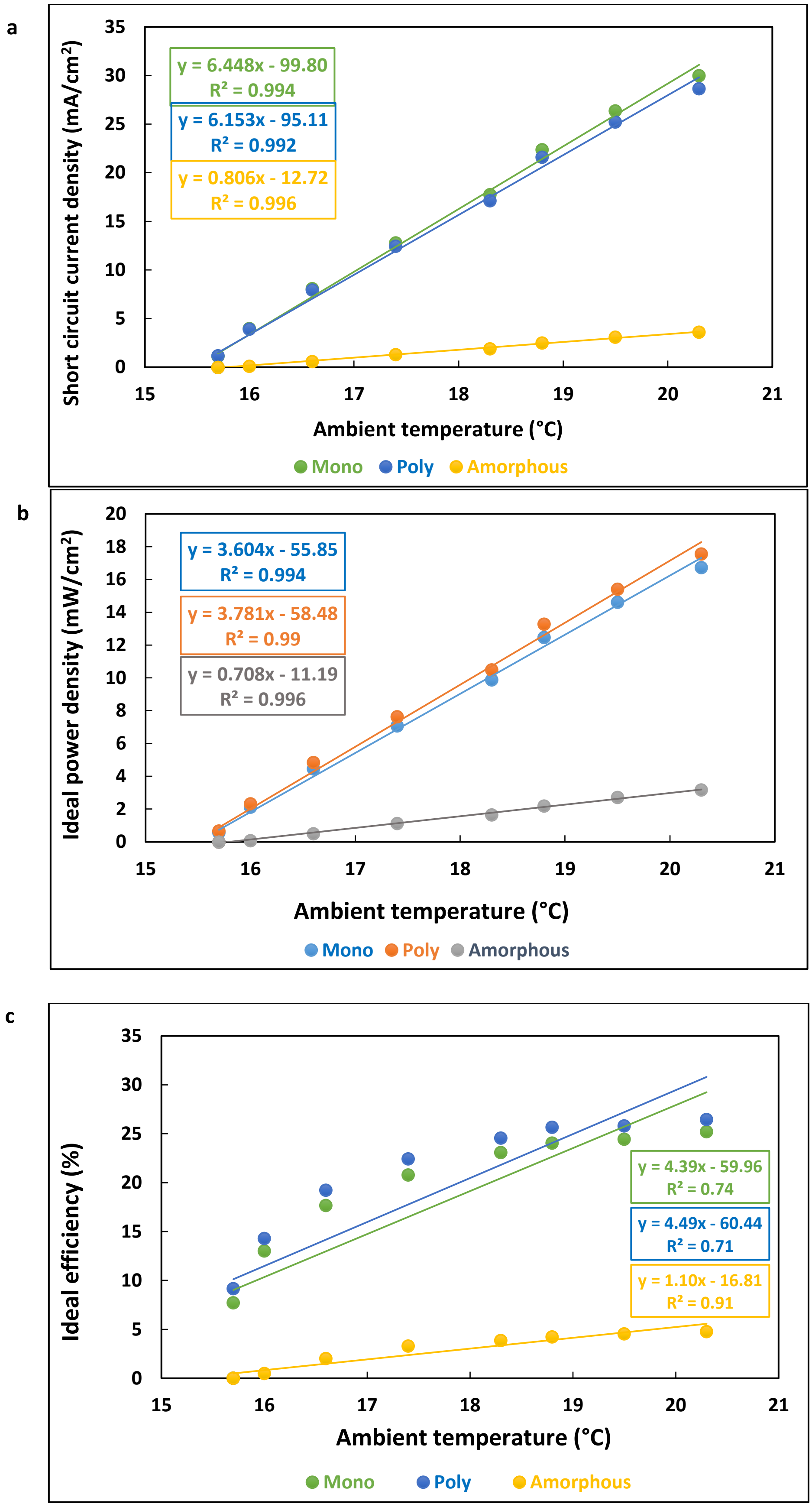


**Figure 5: (a, b, c)** Variations of performance parameters (a) $J_{sc}$ ,(b) $P_D$, and (c) $\eta_o$, of the three modules, mc-Si, pc-Si, and a-Si, with $T_a$ before noon on the experimental day in April

On the contrary, in Figure 6(a), it is noted that the rate of change of $J_{sc}$ varies in an inverse way with the rise in $T_a$ in the afternoon period (from 1:00 p.m. to 4:00 p.m.). As a result of the decreasing rate in $J_{sc}$, it is observed that there is also a depression in $P_D$ and $\eta_o$ with a rise in $T_a$ in the afternoon period, as shown in Figure 6 (b, c), respectively. From Figures 5 and 6, we can clearly observe that all the parameters $J_{sc}$, $P_D$, and $\eta_o$ have the same pattern of variation with $T_a$ in the periods before and afternoon. Also, one can notice that the wafer technologies of mc-Si and pc-Si have a larger rate of change in $J_{sc}$, $P_D$, and $\eta_o$ than a-Si technology with $T_a$ before and afternoon. This can be explained by the fact that mc-Si is more sensitive to temperature than pc-Si, and the least effect of $T_a$ is on a-Si, as stated before [25, 26].

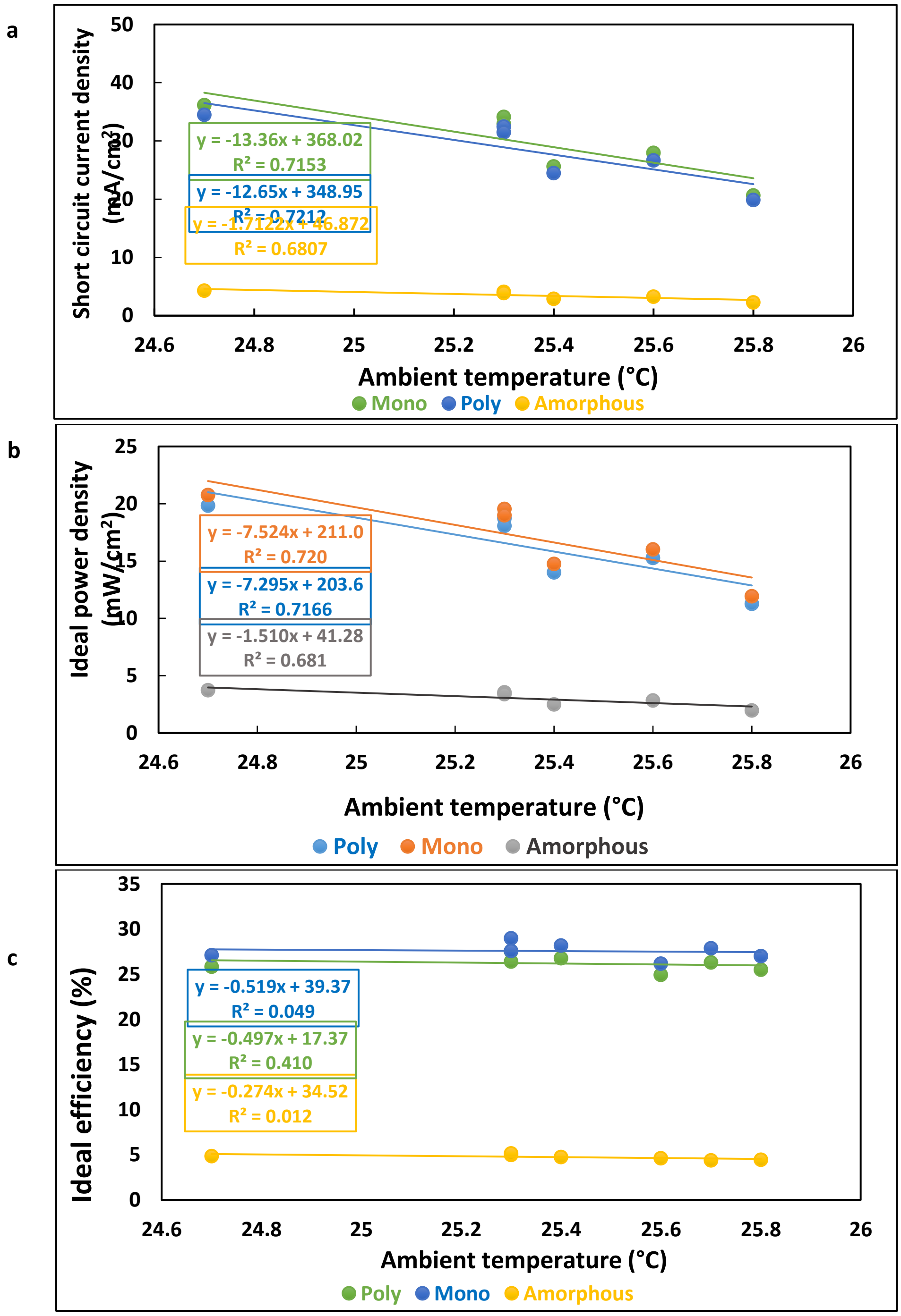


**Figure 6: (a, b, c)** Variations of performance parameters (a) $J_{sc,}$ (b) $P_D$, and (c) $\eta_o$, of the three modules, mc-Si, pc-Si, and a-Si, with $T_a$ in the afternoon in April

On the other hand, Figure 7(a, b) shows the variation of $T_a$ with $\eta_o$ for the three modules mc-Si, pc-Si, and a-Si in the afternoon period from 1:00 p.m. to sunset in detail. As it is clear in Figure 7(a), in the late afternoon after 5 p.m., there is a sudden increase in the efficiencies of mc-Si and pc-Si. This could be attributed to the fact that, during this period of the day, there is a sudden decrease in solar irradiance, which affects the ambient temperature by lowering its value, as reported by [15]. But it can be noted that $\eta_o$ of pc-Si has a larger rate of increase than mc-Si. This is due to the large air mass value during this period, which causes multiple scattering and increases the rate of diffuse irradiance. Hence, a red shift in the short wavelengths towards the long wavelengths occurs, as inferred from Zenhom et al [19]. This leads to more absorption in pc-Si layers than mc-Si [27, 28] and less absorption in a-Si, causing a higher rise in $\eta_o$ of pc-Si than mc-Si and a decrease in $\eta_o$ of a-Si .These results show a great impact of ambient temperature variation on the performance parameters of solar PV modules.

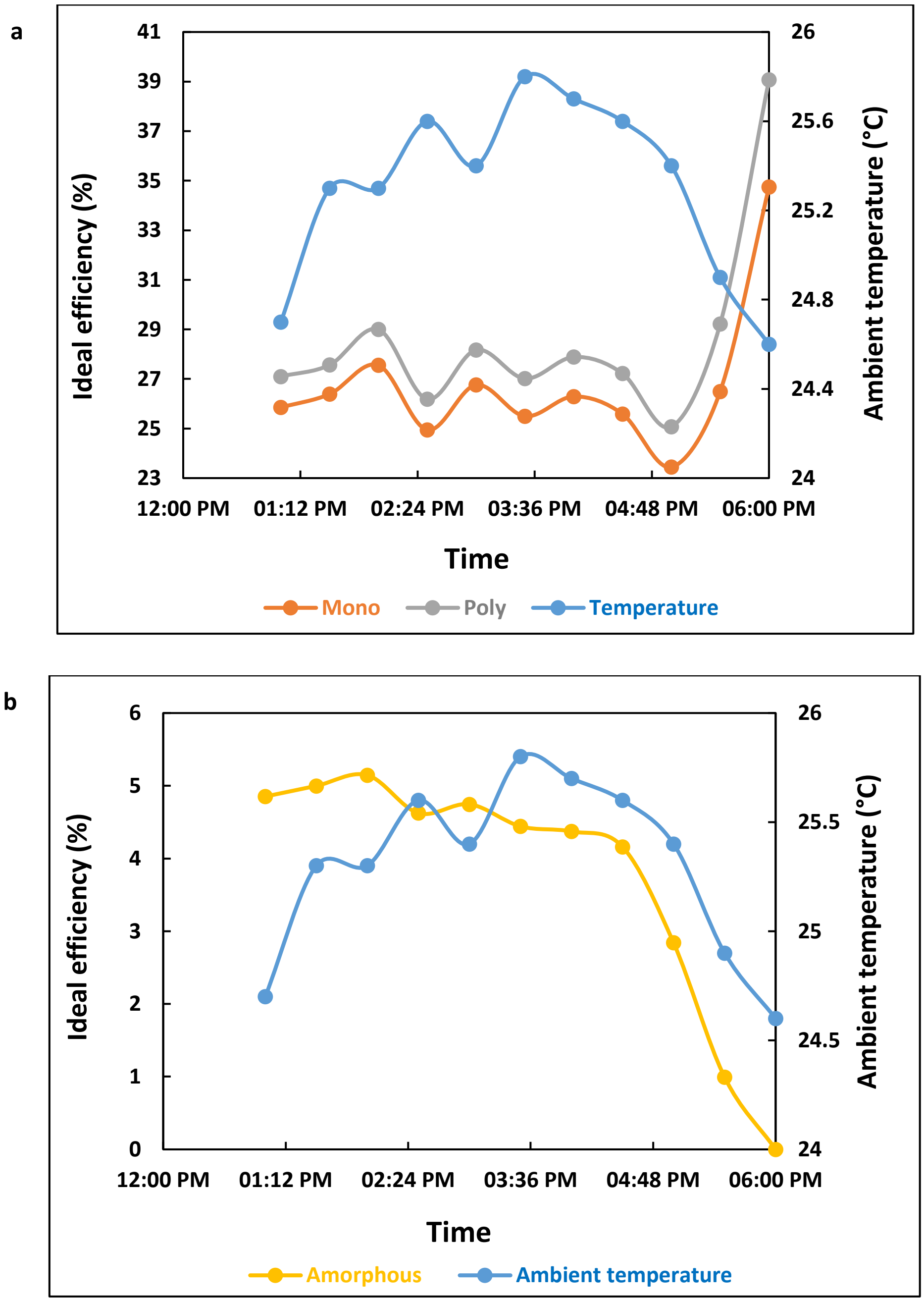


**Figure 7: (a, b)** Variations of $\eta_o$ with $T_a$ for the three modules mc-Si, pc-Si, and a-Si in the afternoon period from 1:00 p.m. to sunset in April

**3.2. Relative humidity dependence of modules' performance parameters**

This section investigates the impact of relative humidity (R.H.) on the performance parameters of the three solar PV modules ($V_{oc}$, $J_{sc}$, $P_D$, and $\eta_o$). Figure 8 reveals how the R.H. and $V_{oc}$ of the three PV modules changed over time in the spring season from sunrise to sunset. It is clear from Figure 8 that the data in the diagram can be split into three periods. Early in the morning, when R.H. falls, $V_{oc}$ of the three modules begins to rise. In contrast, when R.H. drops through midday, the rate of change remains essentially constant due to the maximum capacity voltage. At the end of the day, a dramatic fall in the $V_{oc}$ is then seen, along with a rise in R.H.

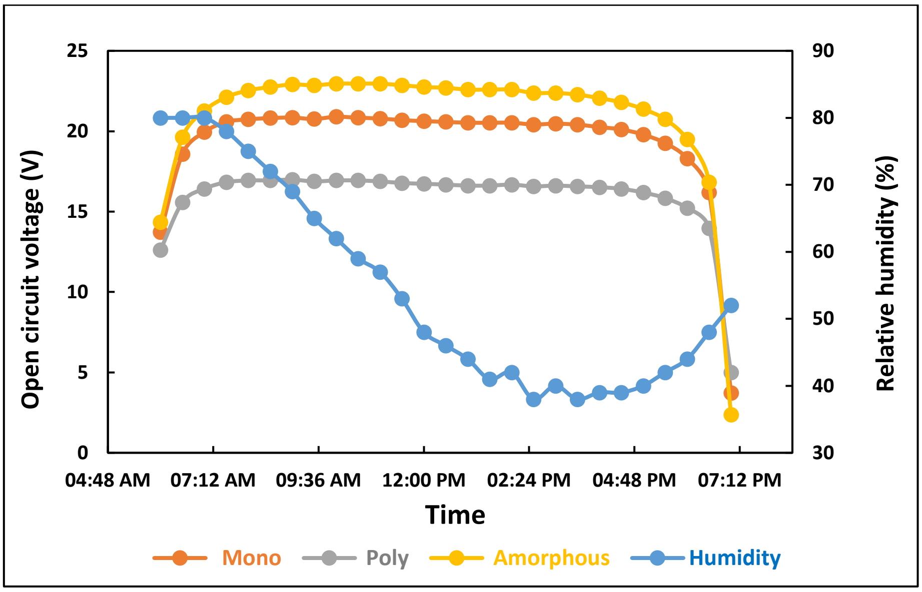


**Figure 8:** Variations of $V_{OC}$ with R.H. for the three modules mc-Si, pc-Si, and a-Si from sunrise to sunset in April

On the other hand, Figure 9 (a, b, c) represents the variation of ($J_{sc}$, $P_D$, and $\eta_o$) with R.H. in the before noon period. It is observed that there is a decreasing trend in ($J_{sc}$, $P_D$, and $\eta_o$) of the three modules when relative humidity increases. This can be explained by the fact that high relative humidity may cause diffraction, reflection, and absorption of solar irradiance. As a result, each solar PV ideal power density $P_D$, and ideal efficiency $\eta_o$ are reduced during the before noon period. These results are in good agreement with previous work [4, 18, 29].

a

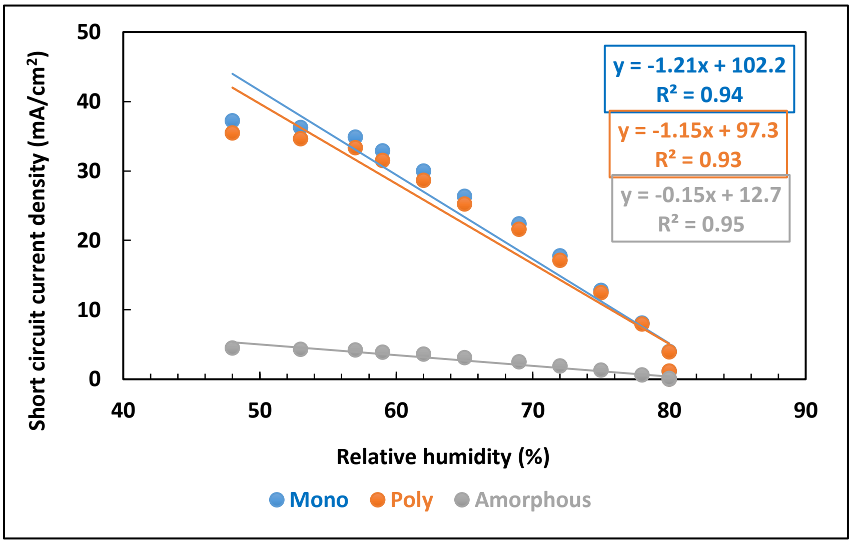

b

c

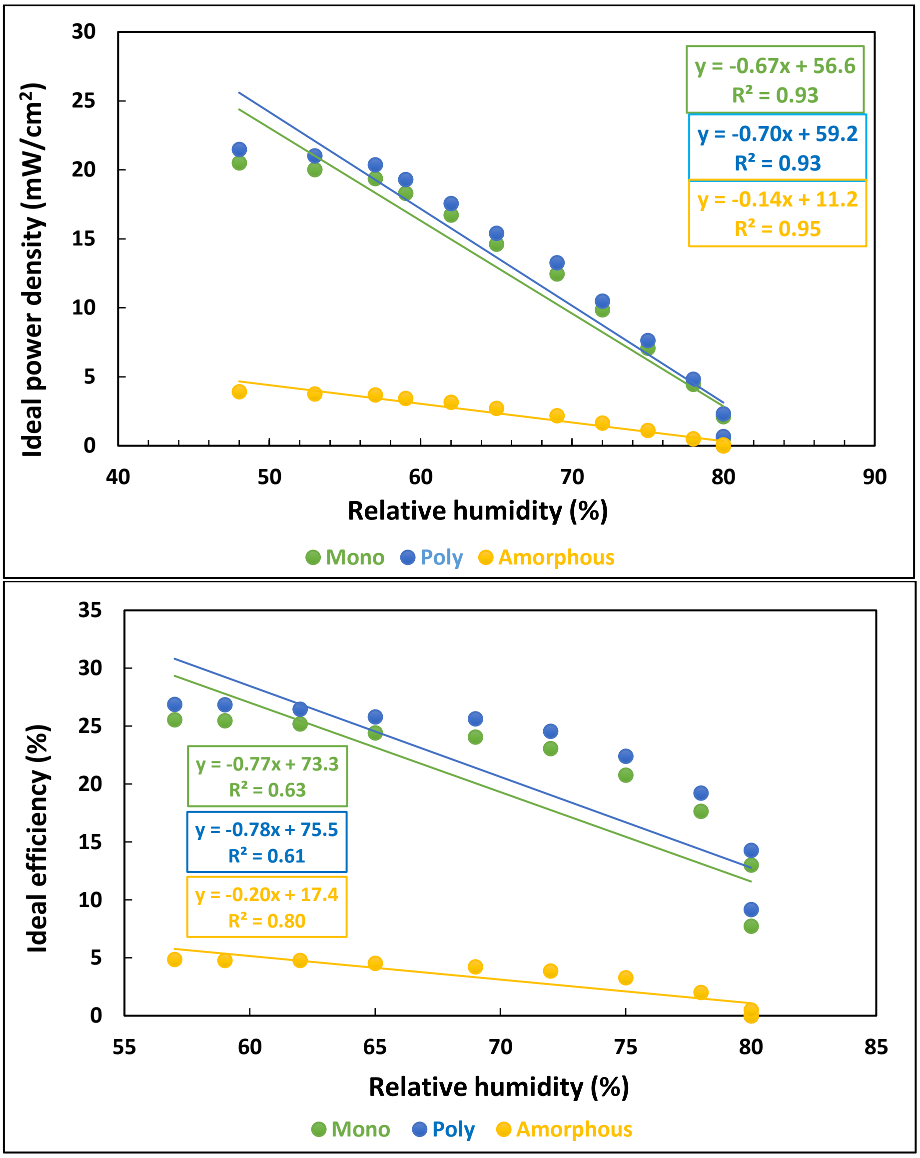


**Figure 9:** (a,b, c) Variations of performance parameters (a) $J_{sc}$ (b), $P_D$, and (c) $\eta_o$, of the three modules, mc-Si, pc-Si, and a-Si, with R. H. in the before noon period in April

Similarly, in the afternoon period of the day, there is an inverse correlation between $J_{sc}$ $P_D$, and $\eta_o$ and R.H. (behavior not presented here). It has been found that the variation in $J_{sc}$ ,$P_D$, and $\eta_o$ of the three modules in the afternoon period slightly differs from that of the before noon period. The thin film technology exhibited a lower rate of decrease in $J_{sc.}$ [30, 31], $P_D$, and $\eta_o$ with humidity compared to the wafer technologies. Increasing humidity affects more mc-Si and pc-Si PV modules than a-Si PV modules. This can be attributed to the spectral changes occurring exactly in the wavelength range where mc-Si and pc-Si PV modules' spectral responses lie [28, 31]. These spectral changes are caused by water vapor, which absorbs IR solar irradiance. On the other hand, these spectral changes do not occur in the wavelength range where the amorphous module's spectral response lies (in the visible range as stated before [25, 28]. Hence, the humidity effect on an amorphous PV module is very weak.

### 3.3. Solar irradiance dependence of modules' performance parameters

In this section, the effect of solar irradiance on modules' performance parameters ($V_{oc}$, $J_{sc}$, $P_D$, and $\eta_o$) is introduced. It has been found that $V_{oc}$ grows exponentially to its maximum value as solar irradiation increases, which is clear in Figure 10. This can be attributed to the fact that when incident light intensity increases, the before-midday $V_{oc}$ of the three distinct PV module technologies also increases. Also, it can be noticed that the rate of increase in $V_{oc}$ with solar irradiance is different. This is because each of the materials used to construct the modules have different physical characteristics, such as temperature coefficients, the ideality factor of the diode, and the diode saturation current [16].

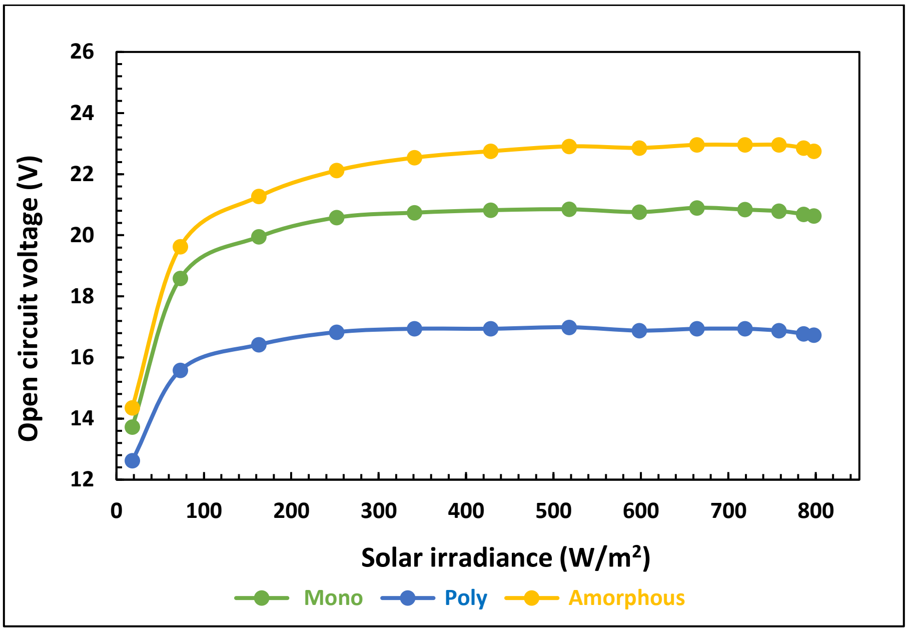


**Figure 10:** Variations of $V_{OC}$ with G for the three modules mc-Si, pc-Si, and a-Si in the afternoon period in April

Figure 11 (a, b, c) shows the impact of irradiance on ($J_{sc}$, $P_D$, and $\eta_o$) in the before noon period of the clear day in the spring season. Figure 11 (a) makes it clear that as the intensity of light increased, each PV module technology had a different increment in $J_{sc}$ depending on its spectral response. However, the behavior of the mc-Si and pc-Si modules was close enough. The fact that monocrystalline crystals are dependent on direct sunlight while polycrystalline crystals are less dependent on direct insolation and can generate energy in diffused light [27], which is the primary atmospheric feature at the Helwan location measures a more steady flow of electricity throughout the day [32]. On the other hand, as we infer from the findings of Zenhom et al. [19], the maximum extinction coefficient caused by pollutants and aerosols present at the Helwan site occur exactly in the wavelength range where the amorphous module's spectral response lies. As a result, the increment value in the $J_{sc}$ of the amorphous module is lower than that of the other two modules. These results are in good agreement with those of Ramgolam et al. [16].

As seen in Figure 11 (b), a PV module's output power is linearly related to the amount of solar radiation hitting its surface. It is clear that the $P_D$ of the three modules increased at a varied rate depending on intensity. It can be observed that $J_{sc}$ and $P_D$ increase with irradiance. These results are in good agreement with those of WanQuan et al. [17]. It can be noted that in Figure 11 (c), the values of $\eta_o$ obtained from the three PV modules slightly increased with an increase in solar irradiance. This can be explained by the increase in incident irradiance with high levels, which leads to an increase in the ambient temperature and more excited electrons. Hence, the possibility of multi-collisions of generated electrons in the forbidden gab increases, hindering the movement of electrons lowering $V_{oc}$ and $\eta_o$. It well means that the solar irradiance during peak sun periods does not necessarily lead PV modules to operate efficiently. The same results have been obtained by Amelia et al., [33].

Similarly, in the afternoon period of the day, there is a direct correlation between $J_{sc}$ and solar irradiance. This direct correlation leads to a reduction in the $P_D$ consequently; $\eta_o$ also decreases as the solar irradiance decreases during the afternoon period (behavior not presented here). It has been found that the variation in $J_{sc}$, $P_D$, and $\eta_o$ of the three modules in the afternoon period slightly differs from that of the before noon period.

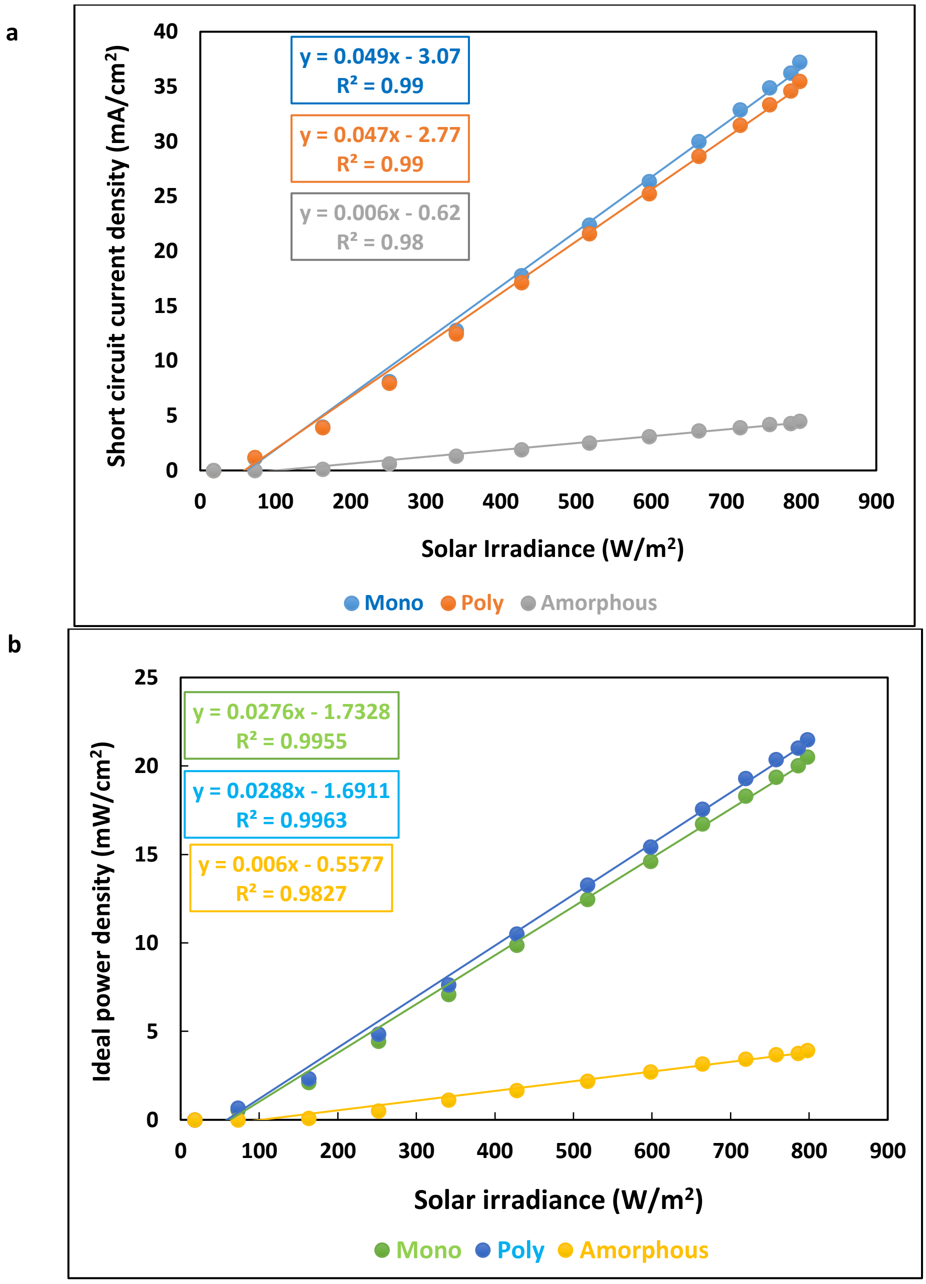

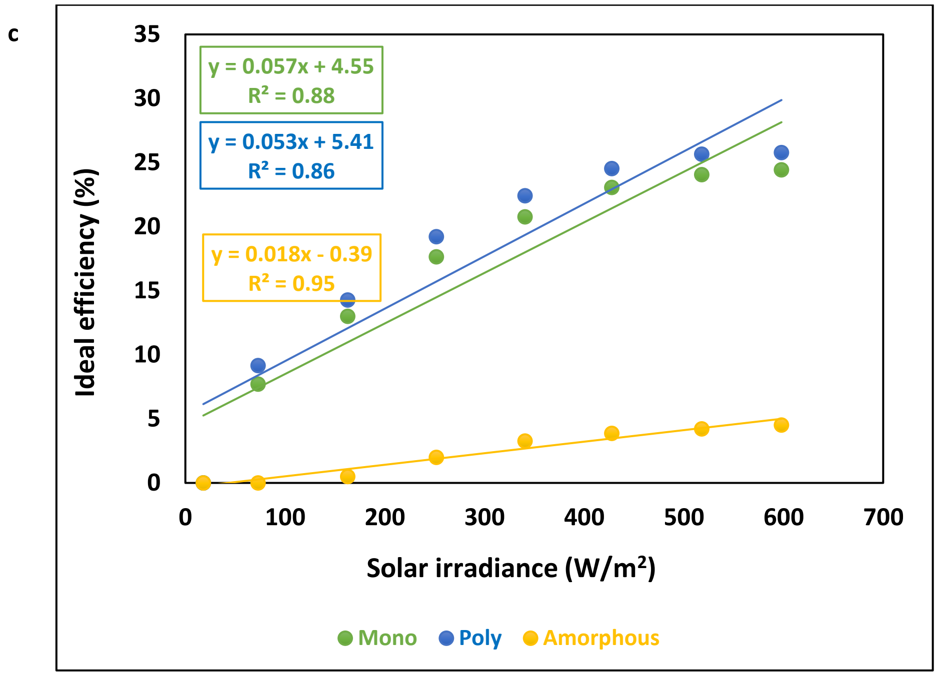


**Figure 11: (a, b, c)** Variations of performance parameters (a) $J_{sc}$ (b), $P_D$, and (c) $\eta_o$, of the three modules, mc-Si, pc-Si, and a-Si, with G in the before noon period in April

**Part II: Description of the obtained results in the four seasons**

Tables 2 to 4 represent the effect of environmental factors $T_a$ °C, R.H. (%), and G (W/m$^2$) on the performance parameters $V_{oc}$, $I_{sc}$, $P_D$, and $\eta_o$, of the three PV modules in the four seasons. The tables show the variation in the performance parameters of the three PV modules in each season during the study period. These tables are obtained by applying linear regression analyses, where $V_{oc}$, $J_{sc}$, $P_D$, and $\eta_o$ are the dependent variables and $T_a$, R.H., and G are the independent variables.

In Table 2 of mc-Si, for the before noon period from sunrise to 10:00 a.m., we found that the $T_a$ affected the $V_{oc}$ in the summer season, having the highest rate of increase of 1.57 V/ºC, while the winter season had the highest rate of increase in ($J_{sc}$) and ($P_D$) of 7.53 mA/cm$^2$ and 4.09 mW/cm$^2$ per unit increase in $T_a$, respectively. As a result, the winter season experienced the biggest growth in ($\eta_o$), which was 6.09%/ºC. On the contrary, during the summer season in the afternoon period from 1:00 p.m. to 4:00 p.m., the maximum depression in the parameters $V_{oc}$, $J_{sc}$, and $P_D$ /°C was obtained, as it is clear in Table 2. The summer had the highest depression in the ($\eta_o$) -0.60%/°C as an outcome. Meanwhile, there was an increase in ($\eta_o$) by 0.88%/°C in the winter season. Since the single crystals of mc-Si are better at transporting heat than the pc-Si and a-Si materials [26]. Hence, mc-Si shows the largest rate of increase and decrease in $J_{sc}$ for all the seasons with ambient temperature.

With respect to R.H., the summer season recorded the lowest rates of decline in the parameters $V_{oc}$, $J_{sc}$, and $P_D$ with the rise in R.H., as shown in Table 2. In this case, the summer season exhibited a decline in ($\eta_o$) of just -0.36%. On the other hand, the parameters $V_{oc}$, $J_{sc}$, and $P_D$ had the highest rates of decrease with increasing R.H. during the winter. In this sense, the winter season showed the greatest percentage drop in $\eta_o$ -0.88%/1% R.H. In terms of (G), this environmental factor had the least impact on the parameters $V_{oc}$, $J_{sc}$, and $P_D$, during the summer season, and in this case, the summer had the lowest rise in ($\eta_o$) by 0.03% /W/m$^2$. While G had the greatest impact on the parameters $V_{oc}$, $J_{sc}$, and $P_D$ in the winter season per unit increase in irradiance, consequently, each unit increase in solar irradiation during the winter can raise $\eta_o$ by 0.06%.

**Table 2: Environmental effects on the performance parameters of the mono-Si module in the four seasons, winter, spring, summer, and autumn**

| Season | Per. Parameters / Env. Factors | $V_{OC}$ (V) | | $J_{SC}$ (mA/cm$^2$) | | $P_D$ (mW/ cm$^2$) | | $\eta_o$ (%) | |
|---|---|---|---|---|---|---|---|---|---|
| Winter | $T_a$ (°C) | b.n | a.n | b.n | a.n | b.n | a.n | b.n | a.n |
| | | 0.07 | -4.26 | 7.53 | -2.80 | 4.09 | -1.59 | 6.09 | 0.88 |
| | R.H. (%) | -0.32 | | -1.65 | | -0.896 | | -0.876 | |
| | G (W/m$^2$) | 0.03 | | 0.06 | | 0.033 | | 0.063 | |
| Spring | $T_a$ (°C) | b.n | a.n | b.n | a.n | b.n | a.n | b.n | a.n |
| | | 0.20 | -5.18 | 6.44 | -13.36 | 3.60 | -7.52 | 4.39 | -0.51 |
| | R.H. (%) | -0.18 | | -1.21 | | -0.672 | | -0.771 | |
| | G (W/m$^2$) | 0.007 | | 0.049 | | 0.027 | | 0.058 | |
| Summer | $T_a$ (°C) | b.n | a.n | b.n | a.n | b.n | a.n | b.n | a.n |
| | | 1.57 | -6.09 | 3.64 | -13.96 | 1.96 | -7.65 | 2.07 | -0.60 |
| | R.H. (%) | -0.03 | | -0.74 | | -0.39 | | -0.37 | |
| | G (W/m$^2$) | 0.002 | | 0.047 | | 0.025 | | 0.03 | |
| Autumn | $T_a$ (°C) | b.n | a.n | b.n | a.n | b.n | a.n | b.n | a.n |
| | | 0.82 | -5.09 | 6.67 | -12.31 | 3.58 | -6.74 | 5.21 | -0.41 |
| | R.H. (%) | -0.26 | | -1.12 | | -0.614 | | -0.727 | |
| | G (W/m$^2$) | 0.012 | | 0.049 | | 0.027 | | 0.0317 | |

Similar findings have been obtained for the other two PV technologies, pc-Si and a-Si, with the exception that each technology has a distinct rate of decline or growth for the parameters $V_{oc}$, $J_{sc}$, $P_D$, and $\eta_o$, as is clear in Tables 3 and 4.
For instance, Table 3 demonstrates that ($\eta_o$) of pc-Si had the most significant increase of 6.61%/ºC in the before noon period, from sunrise to 10:00 a.m., of the winter season. In contrast, the summer exhibited the highest value of depression in ($\eta_o$) for poly-Si [3], with -0.57% /°C specifically in the afternoon period from 1:00 p.m. to 4:00 p.m. On the other hand, $\eta_o$ of pc-Si decreased by the largest percentage (-0.78%) per unit increase in R.H. over the winter season. On the contrary, the winter season showed the greatest percentage increase in $\eta_o$ of pc-Si per unit increase in G by 0.06%.

Table 4 demonstrates that ($\eta_o$) of a-Si technology had the most significant growth of 2.03% / ºC in the before noon period from sunrise to 10:00 a.m. of the winter season. In contrast, the summer exhibited the highest value of depression in ($\eta_o$) for a-Si [9], with -2.0%/°C specifically in the afternoon period from 1:00 p.m. to 4:00 p.m. On the other hand, $\eta_o$ of a-Si decreased by the greatest percentage (-0.32%) per unit increase in R.H. over the winter season. On the contrary, the winter season showed the greatest percentage increase in $\eta_o$ of a-Si per unit increase in G by 0.02%.

**Table 3:** Environmental effects on the performance parameters of the poly-Si module in the four seasons, winter, spring, summer, and autumn

| Season | Per. Parameters / Env. Factors | $V_{OC}$ (V) | | $J_{SC}$ (mA/cm$^2$) | | $P_D$ (mW/ cm$^2$) | | $\eta_o$ (%) | |
|---|---|---|---|---|---|---|---|---|---|
| Winter | $T_a$ (°C) | b.n | a.n | b.n | a.n | b.n | a.n | b.n | a.n |
| | | 0.01 | -2.63 | 7.09 | -2.62 | 4.24 | -1.53 | 6.61 | 1.02 |
| | R.H. (%) | -0.22 | | -1.55 | | -0.928 | | -0.78 | |
| | G (W/m$^2$) | 0.02 | | 0.057 | | 0.034 | | 0.059 | |
| Spring | $T_a$ (°C) | b.n | a.n | b.n | a.n | b.n | a.n | b.n | a.n |
| | | 0.11 | -3.58 | 6.15 | -12.65 | 3.78 | -7.29 | 4.49 | -0.4 |
| | R.H. (%) | -0.11 | | -1.15 | | -0.70 | | -0.784 | |
| | G (W/m$^2$) | 0.004 | | 0.047 | | 0.028 | | 0.054 | |
| Summer | $T_a$ (°C) | b.n | a.n | b.n | a.n | b.n | a.n | b.n | a.n |
| | | 1.00 | -4.52 | 3.45 | -13.13 | 2.03 | -7.39 | 2.12 | -0.57 |
| | R.H. (%) | -0.02 | | -0.70 | | -0.41 | | -0.37 | |
| | G (W/m$^2$) | 0.001 | | 0.045 | | 0.026 | | 0.03 | |
| Autumn | $T_a$ (°C) | b.n | a.n | b.n | a.n | b.n | a.n | b.n | a.n |
| | | 0.49 | -3.52 | 5.88 | -10.92 | 3.69 | -6.54 | 5.56 | -0.37 |
| | R.H. (%) | -0.16 | | -1.00 | | -0.597 | | -0.65 | |
| | G (W/m$^2$) | 0.008 | | 0.044 | | 0.026 | | 0.032 | |

**Table 4:** Environmental effects on the performance parameters of the amorphous-Si module in the four seasons, winter, spring, summer, and autumn

| Season | Per. Parameters / Env. Factors | $V_{OC}$ (V) | | $J_{SC}$ (mA/cm$^2$) | | $P_D$ (mW/ cm$^2$) | | $\eta_o$ (%) | |
|---|---|---|---|---|---|---|---|---|---|
| Winter | $T_a$ (°C) | b.n | a.n | b.n | a.n | b.n | a.n | b.n | a.n |
| | | 0.56 | -5.13 | 0.98 | -0.35 | 0.96 | -0.32 | 2.03 | -0.15 |
| | R.H. (%) | -0.64 | | -0.22 | | -0.188 | | -0.32 | |
| | G (W/m$^2$) | 0.04 | | 0.008 | | 0.007 | | 0.02 | |
| Spring | $T_a$ (°C) | b.n | a.n | b.n | a.n | b.n | a.n | b.n | a.n |
| | | 0.46 | -6.19 | 0.80 | -1.71 | 0.70 | -1.5 | 1.10 | -0.27 |
| | R.H. (%) | -0.25 | | -0.15 | | -0.14 | | -0.20 | |
| | G (W/m$^2$) | 0.009 | | 0.006 | | 0.006 | | 0.02 | |
| Summer | $T_a$ (°C) | b.n | a.n | b.n | a.n | b.n | a.n | b.n | a.n |
| | | 2.98 | -7.30 | 0.44 | -2.55 | 0.33 | -2.08 | 0.41 | -0.3 |
| | R.H. (%) | -0.07 | | -0.09 | | -0.007 | | -0.07 | |
| | G (W/m$^2$) | 0.005 | | 0.006 | | 0.004 | | 0.005 | |
| Autumn | $T_a$ (°C) | b.n | a.n | b.n | a.n | b.n | a.n | b.n | a.n |
| | | 1.09 | -6.11 | 1.19 | -2.44 | 0.84 | -1.96 | 1.80 | -0.2 |
| | R.H. (%) | -0.51 | | -0.21 | | -0.171 | | -0.27 | |
| | G (W/m$^2$) | 0.023 | | 0.009 | | 0.007 | | 0.009 | |

## Conclusion

In the present work, the influence of environmental factors (ambient temperature Ta, relative humidity R.H., and solar irradiance G) on the performance parameters (open circuit voltage Voc, short circuit current density Jsc, ideal output power density PD, and ideal efficiency ηo) of three solar PV mc, pc-Si, and a-Si modules has been studied. The study employed the first-designed NRIAG I-V logger as a prototype for data collection in Helwan site. The results revealed that there was a performance difference among the three PV modules during the four seasons of 2021. In this sense, it has been found that the performance difference was strongly dependent on the seasonal ideal efficiency $\eta_o$ variation of the three PV modules. It has been found that $\eta_o$ of mc-Si, pc-Si, and a-Si were increased by approximately 2.07 to 6.09%, 2.1 to 6.6%, and 0.41 to 2.03%, respectively, corresponding to the effect of $T_a$ in the before noon period of the four seasons. On the contrary, $\eta_o$ of mc-Si, pc-Si, and a-Si were decreased by approximately 0.4 to 0.6%, 0.37 to 0.57%, and 0.15 to 0.3%, respectively, corresponding to the effect of $T_a$ in the afternoon period of the four seasons.

Furthermore, relative humidity (R.H.) changes between winter and summer were remarkable and were especially important for lower band gap devices like mc-Si and pc-Si materials. Therefore, R.H. was considered a major contributor to the seasonal $\eta_o$ variation of -0.37% to -0.87% and -0.37 to -0.78% of mc-Si and pc-Si PV modules, respectively. The R.H. effect on large band gap materials like a-Si was very weak. ($\eta_o$ varies from 0.07% to 0.32% between seasons.)

For low-band gap material-based PV modules like mc-Si and pc-Si materials, $\eta_o$ varied from 0.03% to 0.06% and 0.03% to 0.06% between seasons, respectively, due to the solar irradiance effect. But for large band gap materials like a-Si, the $\eta_o$ varied from 0.005% to 0.02% between seasons.

Finally, it can be concluded that the $\eta_o$ of three PV modules decreased with high air temperatures and high relative humidity while being enhanced slightly with higher solar irradiation. Hence, it is inferred from this study that $T_a$ had the greatest impact on the performance of the three PV modules, in the afternoon period in the summer season. While R.H. had the highest effect on the performance of the three PV modules in the winter season. Also, the performance comparison shows that the performance of pc-Si PV technology was better than that of mc-Si and a-Si PV technology for this location. This can be attributed to the fact that pc-Si crystals can generate energy in diffused light, which is the primary atmospheric feature at the Helwan site and ensures a steadier flow of electricity throughout the day.

## References

**[1]** [1] O. Aljawi, G. Gopir, W. Kamil, and N. S. Mohamad, "Measurement of atmospheric extinction coefficient in the visible spectral region at Bangi, Malaysia," in *AIP Conference Proceedings*, 2016.

**[2]** P.-S. Wei, Y.-C. Hsieh, H.-H. Chiu, D.-L. Yen, C. Lee, Y.-C. Tsai, and T.-C. Ting, "Absorption coefficient of carbon dioxide across atmospheric troposphere layer," *Heliyon,* vol. 4, p. e00785, 2018/10/01/ 2018.

**[3]** M. S. Vasisht, J. Srinivasan, and S. K. Ramasesha, "Performance of solar photovoltaic installations: Effect of seasonal variations," *Solar Energy,* vol. 131, pp. 39-46, 2016.

**[4]** S. Ghazi and K. Ip, "The effect of weather conditions on the efficiency of PV panels in the southeast of UK," *Renewable Energy,* vol. 69, pp. 50-59, 2014.

**[5]** W. Okullo, M. Munji, F. Vorster, and E. Van Dyk, "Effects of spectral variation on the device performance of copper indium diselenide and multi-crystalline silicon photovoltaic modules," *Solar Energy Materials and Solar Cells,* vol. 95, pp. 759-764, 2011.

**[6]** R. Eke and T. R. Betts, "Spectral irradiance effects on the outdoor performance of photovoltaic modules," *Renewable and Sustainable Energy Reviews*, vol. 69, pp. 429-434, 2017.
**[7]** K. Nishioka, T. Hatayama, Y. Uraoka, T. Fuyuki, R. Hagihara, and M. Watanabe, "Field-test analysis of PV system output characteristics focusing on module temperature," *Solar Energy Materials and Solar Cells*, vol. 75, pp. 665-671, 2003.
**[8]** S. Choi, T. Ishii, R. Sato, Y. Chiba, and A. Masuda, "Performance degradation due to outdoor exposure and seasonal variation in amorphous silicon photovoltaic modules," *Thin Solid Films,* vol. 661, pp. 116-121, 2018.
**[9]** E. Alhamer, A. Grigsby, and R. Mulford, "The Influence of Seasonal Cloud Cover, Ambient Temperature and Seasonal Variations in Daylight Hours on the Optimal PV Panel Tilt Angle in the United States," *Energies*, vol. 15, p. 7516, 2022.
**[10]** S. A. Said, G. Hassan, H. M. Walwil, and N. Al-Aqeeli, "The effect of environmental factors and dust accumulation on photovoltaic modules and dust-accumulation mitigation strategies," *Renewable and Sustainable Energy Reviews*, vol. 82, pp. 743-760, 2018.
**[11]** T. Bhattacharya, A. K. Chakraborty, and K. Pal, "Effects of ambient temperature and wind speed on performance of monocrystalline solar photovoltaic module in Tripura, India," *Journal of Solar Energy,* vol. 2014, 2014.
**[12]** W. Mariam and S. Husni, "Influence of malaysian climate on the efficiency of polycrystalline solar cells," in *2006 IEEE International Power and Energy Conference*, 2006, pp. 54-57.
**[13]** H. Zitouni, A. A. Merrouni, M. Regragui, A. Bouaichi, C. Hajjaj, A. Ghennioui, and B. Ikken, "Experimental investigation of the soiling effect on the performance of monocrystalline photovoltaic systems," *Energy Procedia*, vol. 157, pp. 1011-1021, 2019.
**[14]** F. A. Touati, M. A. Al-Hitmi, and H. J. Bouchech, "Study of the effects of dust, relative humidity, and temperature on solar PV performance in Doha: comparison between monocrystalline and amorphous PVS," *International journal of green energy,* vol. 10, pp. 680-689, 2013.
**[15]** M. A. Bashir, H. M. Ali, S. Khalil, M. Ali, and A. M. Siddiqui, "Comparison of performance measurements of photovoltaic modules during winter months in Taxila, Pakistan," *International Journal of Photoenergy,* vol. 2014, 2014.
**[16]** Y. K. Ramgolam and K. Bangarigadu, "Simple and effective method for evaluating performance of Si based photovoltaic cell technologies," *AIMS Energy*, vol. 6, 2018.
**[17]** S. WanQuan, E. Niringiyimana, and V. Ndayishimiye, "Analysis of electrical characteristics and performance of poly-crystalline solar PV module by IV tester under temperature and solar irradiance variation in spring season," in *2020 IEEE PES/IAS PowerAfrica*, 2020, pp. 1-5.
**[18]** J. Tijjani, B. Hamza, and S. Igwenagu, "The effect of humidity and temperature on the efficiency of solar power panel output in Dutsin-ma local government area (LGA), Nigeria," *Journal of Asian Scientific Research*, vol. 10, pp. 1-16, 2020.
**[19]** H. Zenhom, A. Ghitas, M. M. Abdelwahab, M. S. Alnawawy, A. H. Hassan, and A. Abulwfa, "Impact of atmospheric extinction coefficient on the solar spectrum at selective wavelengths at Helwan in Egypt," in *IOP Conference Series: Materials Science and Engineering*, 2022, p. 012011.
**[20]** M. R. Gomaa, R. J. Mustafa, and H. Rezk, "An experimental implementation and testing of a concentrated hybrid photovoltaic/thermal system with monocrystalline solar cells using linear Fresnel reflected mirrors," *International Journal of Energy Research,* vol. 43, pp. 8660-8673, 2019.
**[21]** A. Ndiaye, C. M. Kébé, P. A. Ndiaye, A. Charki, A. Kobi, and V. Sambou, "Impact of dust on the photovoltaic (PV) modules characteristics after an exposition year in Sahelian environment: The case of Senegal," *International Journal of Physical Sciences*, vol. 8, pp. 1166-1173, 2013.
**[22]** H. Rezk, Z. M. Ali, O. Abdalla, O. Younis, M. R. Gomaa, and M. Hashim, "Hybrid moth-flame optimization algorithm and incremental conductance for tracking maximum power of solar PV/thermoelectric system under different conditions," *Mathematics,* vol. 7, p. 875, 2019.
**[23]** P. Singh, S. Singh, M. Lal, and M. Husain, "Temperature dependence of I–V characteristics and performance parameters of silicon solar cell," *Solar Energy Materials and Solar Cells,* vol. 92, pp. 1611-1616, 2008.
**[24]** P. Singh and N. M. Ravindra, "Temperature dependence of solar cell performance—an analysis," *Solar Energy Materials and Solar Cells,* vol. 101, pp. 36-45, 2012.

**[25]** H. Kang, "Crystalline silicon vs. amorphous silicon: The significance of structural differences in photovoltaic applications," in *IOP Conference Series: Earth and Environmental Science*, 2021, p. 012001.

**[26]** H. Koffi, V. Kakane, A. Kuditcher, A. Hughes, M. Adeleye, and J. Amuzu, "Seasonal variations in the operating temperature of silicon solar panels in southern Ghana," *African Journal of Science, Technology, Innovation and Development,* vol. 7, pp. 485-490, 2015.

**[27]** R. Dallaev, T. Pisarenko, N. Papež, and V. Holcman, "Overview of the Current State of Flexible Solar Panels and Photovoltaic Materials," *Materials,* vol. 16, p. 5839, 2023.

**[28]** A. K. Berwal, N. Kumari, I. Kaur, S. Kumar, and A. Haleem, "Investigating the effect of spectral variations on the performance of monocrystalline, polycrystalline and amorphous silicon solar cells," *Journal of Alternate Energy Sources and Technologies,* vol. 7, pp. 28-36p, 2016.

**[29]** A. L. Bonkaney, S. Madougou, and R. Adamou, "Impact of climatic parameters on the performance of solar photovoltaic (PV) module in Niamey," *Smart Grid and Renewable Energy,* vol. 8, p. 379, 2017.

**[30]** D. S. A. Ahmad, A. Zafar, S. Afzal, H. Anjum, and S. Iqbal, "Impact of Environmental Factors on the Working of Photovoltaic Cells," *American Scientific Research Journal for Engineering, Technology, and Sciences,* vol. 22, pp. 26-31, 2016.

**[31]** M. Chegaar and P. Mialhe, "Effect of atmospheric parameters on the silicon solar cells performance," *Journal of Electron Devices,* vol. 6, 2008.

**[32]** H. K. Elminir, V. Benda, and J. Tousek, "Effects of solar irradiation conditions and other factors on the outdoor performance of photovoltaic modules," *JOURNAL OF ELECTRICAL ENGINEERING-BRATISLAVA-,* vol. 52, pp. 125-133, 2001.

**[33]** A. Amelia, Y. Irwan, W. Leow, M. Irwanto, I. Safwati, and M. Zhafarina, "Investigation of the effect temperature on photovoltaic (PV) panel output performance," *Int. J. Adv. Sci. Eng. Inf. Technol,* vol. 6, pp. 682-688, 2016.